*International Journal of Latest Research in Engineering and Technology (IJLRET)*
*ISSN: 2454-5031*
*www.ijlret.com || Volume 06 - Issue 09 || September 2020 || PP. 55-71*

# Modeling of the thermal fluid flow in stationary plasma arc cutting

Atilla Savaş
*(Mechanical Engineering Department, Piri Reis University, Turkey)*

**Abstract:** This work aims to analyze the thermal fluid flow in a stationary plasma arc cutting operation under the plasma gases argon, air and nitrogen. COMSOL software was utilized to solve multiphysics phenomena, including the laminar flow, the heat transfer, the electric and the magnetic field. The validation of the procedure was confirmed against papers found in the literature. The comparisons showed a good match.
When the plasma behavior of the plasma arc cutting operation is investigated, one can see that physical plasma constriction causes plasmas to flow faster in greater temperatures. The highest plasma inlet velocity makes the most stable arc in argon plasma arc whereas the lowest plasma inlet velocity causes the same result in air plasma arc. Plasma arc torch design can be performed with the proposed method in this work.
**Keywords:** Numerical Simulation, Plasma Arc Cutting, Plasma Constriction

## 1. Introduction

Plasma Arc Cutting (PAC) operation is based on the generation of a plasma arc between the torch cathode and the workpiece acting as an anode, with the high energy and momentum flux rates required to produce a local melting and vaporization in the material, followed by the removal of material. This is achieved by using a narrow copper nozzle that constricts the plasma jet, increasing its maximum temperature and flux velocity. Temperatures over 25 000 K and supersonic velocities are routinely reached in the plasma column generated by these devices [1].

There are a lot of studies investigating the arc behavior of Gas Tungsten Arc Welding (GWAW). In these studies, free burning GTAW arc was analyzed. The first attempt to simulate the GTAW arc was made by Hsu ,Etemadi and Fender [2]. Following attempts by Hsu et al. to validate their own model, McKelliget and Szekelly improved the model to account for the anode and cathode interface layers [3]. Goodarzi, Choo and Toguri took into account the angle of the cathode tip and found that a sharpened electrode increased the velocity of the plasma and thus the contribution of the convective heat flow [4]. Ramirez, Trapaga and McKelliget used two different approaches to simulate the GTAW arc and found that the potential approach provided better results than the magnetic approach [5]. Wu, Ushio and Tanaka (1997) achieved a two-way coupling between the arc and the anode surface [6]. Murphy, Tanaka, Yamamoto, Tashiro, Sato and Lowke modeled the arc under various shielding gases and also considered the metal vapor [7].

There are studies that focus on the PAC and Plasma Arc Welding (PAW) operations. Aguilar, Sanjurjo, Yunta and Calderon built a model to investigate the constricted arc velocity and temperature under air plasma during PAC operation [1]. They did not try other plasma gases in their work. Yin, Hu, Yu and Li also prepared a two-dimensional model to investigate the constricted argon arc [8]. They also did not take into consideration other plasma gases.

In this present study, a two-dimensional axially symmetric model was realized and three different plasma gases were investigated. The temperature and velocity profiles under air, nitrogen and argon plasmas and the arc voltages were calculated. The nozzle radius was changed to analyze the effect of physical constriction of the arc.

## 2. Mathematical Modeling

The plasma arc cutting graphic is depicted in Fig. 1a and the computation domain is shown in Fig.1b. DC electrode negative (DCEN) method is used, the tungsten electrode (argon arc) and the cupper-hafnium electrode (air and nitrogen arcs) are the cathode and the steel workpiece is the anode.

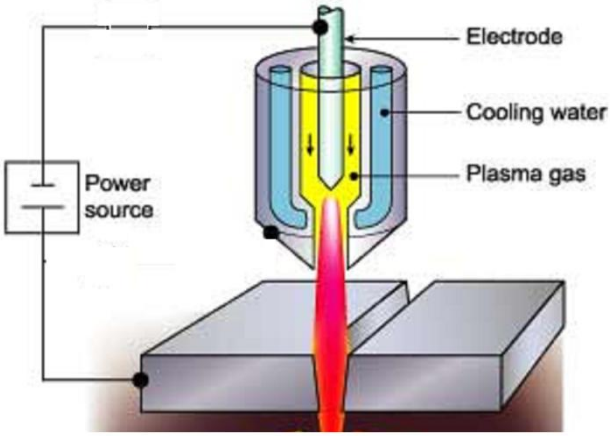


Fig 1a Plasma Arc Cutting Graphic

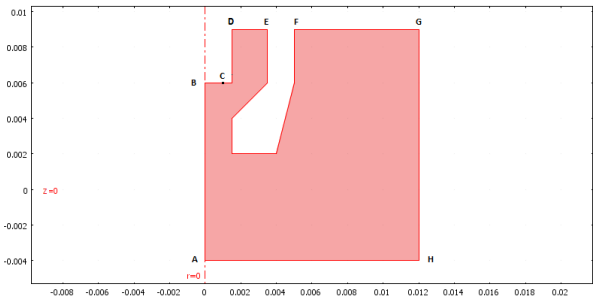


Fig. 1b. Computational Domain for the PAW Arc. (Dimensions are in meters)

**2.1 Assumptions**

- The arc is stationary and under atmospheric pressure, there is no movement for the torch.
- The problem is solved in steady state, terms that include time is canceled
- Gas flow is laminar and incompressible, no turbulence is considered.
- The arc plasma is in Local Thermodynamic Equilibrium (LTE).
- The arc plasma is optically thin, meaning that no absorption is taking place inside the arc.
- Gas properties change only with the temperature.
- Net Emission Coefficient (NEC) method is used to simulate the radiation loss.

**2.2 Governing equations (taken from ref. [11])**

The conservation equations are written as follows:

Mass continuity equation is

$$\frac{\partial}{\partial z}(\rho v)+\frac{1}{r}\frac{\partial}{\partial r}(\rho r u)=0 \tag{1}$$

Here ρ represents mass density; u and v represent radial and axial velocity components.

Radial momentum conservation equation is

$$\frac{\partial}{\partial z}(\rho v u)+\frac{1}{r}\frac{\partial}{\partial r}(\rho r u u)=-\frac{\partial P}{\partial r}+\frac{\partial}{\partial z}\left(\mu\frac{\partial u}{\partial z}+\mu\frac{\partial v}{\partial r}\right)+\frac{1}{r}\frac{\partial}{\partial r}\left(2r\mu\frac{\partial u}{\partial r}\right)-J_z B_\theta \tag{2}$$

Axial momentum conservation equation is

$$\frac{\partial}{\partial z}(\rho v v)+\frac{1}{r}\frac{\partial}{\partial r}(\rho r u v)=-\frac{\partial P}{\partial z}+\frac{\partial}{\partial z}\left(2\mu\frac{\partial v}{\partial z}\right)+\frac{1}{r}\frac{\partial}{\partial r}\left(r\mu\frac{\partial v}{\partial r}+r\mu\frac{\partial u}{\partial z}\right)+J_r B_\theta \tag{3}$$

Here P is pressure, μ is viscosity, $J_r$ and $J_z$ are radial and axial components of current density and $B_\theta$ is the circumferential component of magnetic flux density.

The energy conservation equation is

$$\frac{\partial}{\partial z}\left(\rho v C_p T\right)+\frac{1}{r}\frac{\partial}{\partial r}\left(\rho r u C_p T\right)=\frac{\partial}{\partial z}\left(k\frac{\partial T}{\partial z}\right)+\frac{1}{r}\frac{\partial}{\partial r}\left(rk\frac{\partial T}{\partial r}\right)$$
$$+\frac{J_z^2+J_r^2}{\sigma}-S_R+\frac{5}{2}\frac{k_b}{e}\left(J_z\frac{\partial T}{\partial z}+J_r\frac{\partial T}{\partial r}\right) \quad (4)$$

Here Cp is the heat capacity under constant pressure, k is the heat conductivity, σ is the electrical conductivity, $k_b$ is the Boltzman's constant and e is the elementary electronic charge. The last three terms in the energy conservation equation represent the Joule heating, radiation loss and power done by the electron flux, respectively.

The current continuity equation is

$$\frac{\partial}{\partial z}\left(\sigma\frac{\partial \phi}{\partial z}\right)+\frac{1}{r}\frac{\partial}{\partial r}\left(r\sigma\frac{\partial \phi}{\partial r}\right)=0 \quad (5)$$

Ohm's law can be written as

$$J_z=-\sigma\frac{\partial \phi}{\partial z} \quad (6)$$

$$J_r=-\sigma\frac{\partial \phi}{\partial r} \quad (7)$$

The azimuthal component of the self-induced magnetic field $B_\theta$ is deduced from the magnetic potential components as follows:

$$\frac{\partial^2 A_z}{\partial z^2}+\frac{1}{r}\frac{\partial}{\partial r}\left(r\frac{\partial A_z}{\partial r}\right)=\mu_0 J_z \quad (8)$$

$$\frac{\partial^2 A_r}{\partial z^2}+\frac{1}{r}\frac{\partial}{\partial r}\left(r\frac{\partial A_r}{\partial r}\right)-\frac{A_z}{r^2}=\mu_0 J_r \quad (9)$$

and

$$B_\theta=\frac{\partial A_r}{\partial z}-\frac{\partial A_z}{\partial r} \quad (10)$$

Here φ is the electrical potential and $\mu_0$ is the magnetic permeability of free space. $A_r$ and $A_z$ are the magnetic potential radial and axial components, respectively.

### 2.3 Boundary Conditions(taken from ref. [11])

The boundary conditions are given in Table 1. The plasma gas velocity is taken as 1 m/s. This value corresponds to a flow rate of 1.885 l/min. To analyze the effect of flow rate in some calculations the plasma gas velocity was raised to 7 m/s by 1 m/s increments. The most important boundary condition is the one defined on the line BC in Fig. 1b, which forms the cathode spot. The current density value on this boundary is taken as $J_c$ =6.5x 107 A/$m^2$ ($J_c$ is the cathode current density) no matter what the current value is. The different current values are applied as changing cathode spot radius ($R_c$) as shown in the following equations:

$$J_z=J_c \qquad r<R_c \quad (11)$$

$$J_z=0 \qquad r>R_c \quad (12)$$

$$R_c=\sqrt{\frac{I}{\pi J_c}} \quad (13)$$

Here I is the applied current value in Amperes.

Table 1. The Boundary Conditions

| | Velocity, Pressure | Heat Transfer | Maxwell Equation |
|---|---|---|---|
| BC | Wall condition<br>u=0, v=0 m/sec | 3000 K Tungsten<br>1500 K Hafnium | Magnetic ins. and<br>Current density $J_c$=-6.5x $10^7$ A/$m^2$ |
| CD | Wall condition<br>u=0, v=0 m/sec | 3000 K Tungsten<br>1500 K Hafnium | Magnetic and electric ins. |
| DE | u=0, v=-shielding gas velocity | 500 K | Magnetic and electric ins. |
| EF | Wall condition<br>u=0, v=0 m/sec | 500 K | Magnetic and electric ins. |
| FG | Atmospheric pres.<br>101325 Pascal | 500 K | Magnetic and electric ins. |
| GH | Atmospheric pres.<br>101325 Pascal | 500 K | Magnetic and electric ins. |
| AH | Wall condition<br>u=0, v=0 m/sec | Thermal insulation | Magnetic and electric and ground |
| AB | Axial symmetry | Axial symmetry | Axial symmetry |

**2.4 Properties of gases**

Thermodynamic properties and the transport coefficients of the gases argon, nitrogen and air are taken from Boulos, Fauchais and Pfender [9]. NEC of argon is taken from Evans and Tankin [10]. NEC of other gases is assumed to be the same as that of argon because of lack of data. All of these data are shown in Fig. 2.

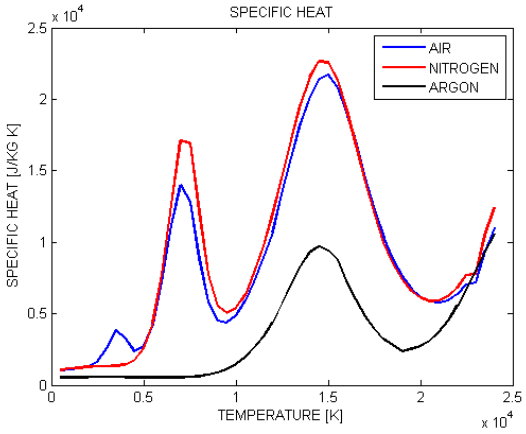


2.a.

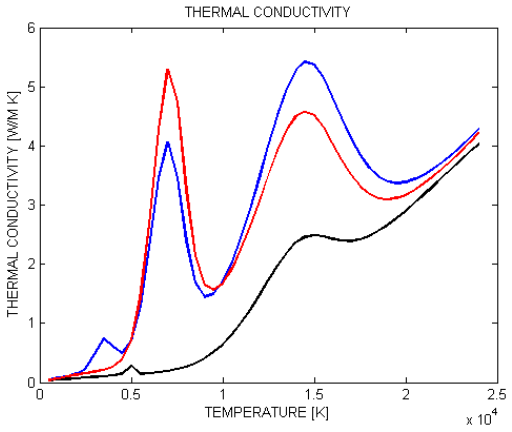


2.b.

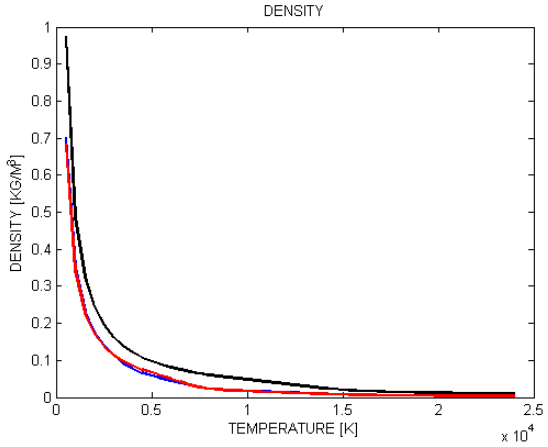
DENSITY
DENSITY [KG/M³]
TEMPERATURE [K]
x 10^4

2.c.

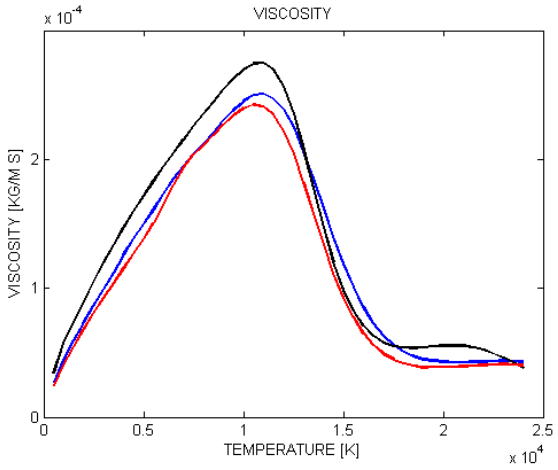
VISCOSITY
x 10^-4
VISCOSITY [KG/M S]
TEMPERATURE [K]
x 10^4

2.d.

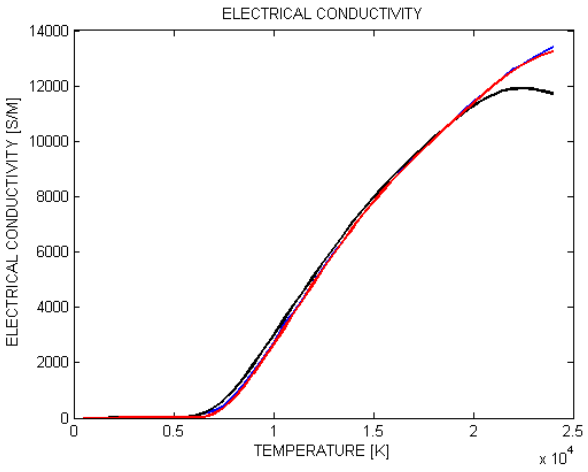
ELECTRICAL CONDUCTIVITY
ELECTRICAL CONDUCTIVITY [S/M]
TEMPERATURE [K]
x 10^4

2.e.

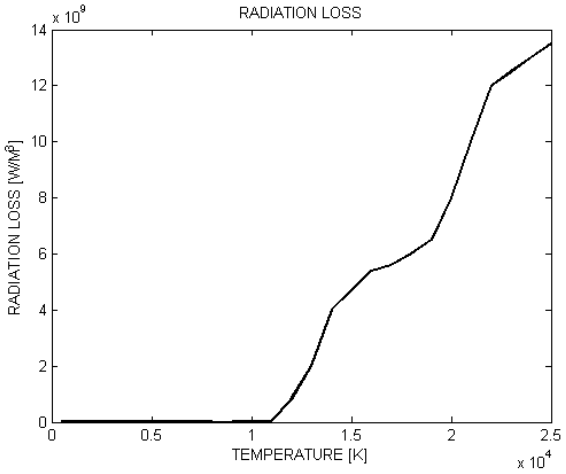


2.f

Fig. 2. Physical Properties of Plasma Gases as a Function of Temperature. a. Specific Heat, b. Thermal Conductivity, c. Density, d. Viscosity, e. Electrical Conductivity, f. Radiation Loss

**2.5 Numerical method**

The numerical method used in this work is adopted from the work of Savaş and Ceyhun [11].

Conservation equations are solved simultaneously to get the velocity and temperature profile of the plasma arc and the voltage drop in the arc. In GTAW arc there is only the magneto hydrodynamic (MHD) constriction. In this present work other than the MHD constriction there is also a physical constriction exerted by the nozzle of the torch to the plasma arc. Since the anode and cathode sheathes are not considered, the heat flux and the current density calculations are not included.

## 3. Results and Discussion

**3.1. Validation According to the Experiments and Numerical Studies in Literature.**

**3.1.1. Experimental and numerical study of Hsu, Etemadi and Pfender [2].**

The temperature profile obtained by Hsu, Etemadi and Pfender coincides with the temperature profile obtained from our model under the same conditions. A visual comparison of our model (right side) with that obtained by Hsu et al. (left side) is presented in Fig. 3a. Discrepancies between the two approaches appear at the arc fringes where the LTE assumption does not prevail. The discrepancy near the anode may be caused by the insulation boundary condition defined on the anode surface. The plasma velocity comparison with Hsu et al.'s numerical work is given in Fig. 3b. The plasma velocity of physically unconstricted argon arc is given in Fig. 4.

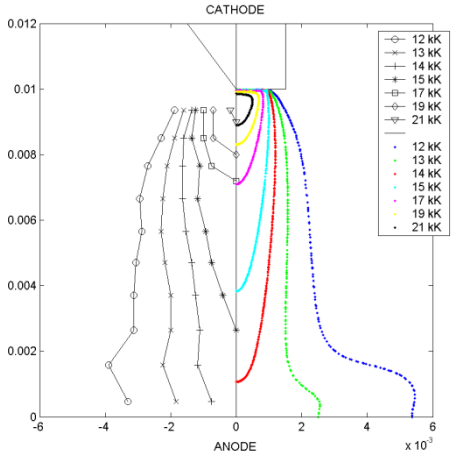


Fig. 3a. Comparison Between Experimental and Calculated Temperature Contours in the Welding Arc for Argon Arc. The Experimental Results (200 A at 10 mm Arc Length) are from Hsu, Etemadi and Pfender [2,11]

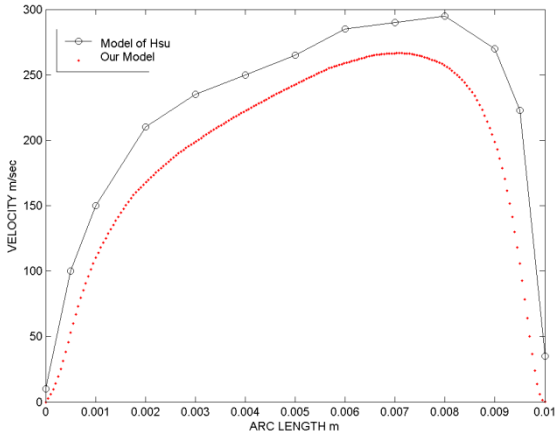


Fig. 3b. Comparison between the Velocity Profiles along the Symmetry Axis from a Numerical Solution in the Literature and our Solution. The Numerical Results (200 A at 10 mm Arc Length) are from Hsu, Etemadi and Pfender [2,11]

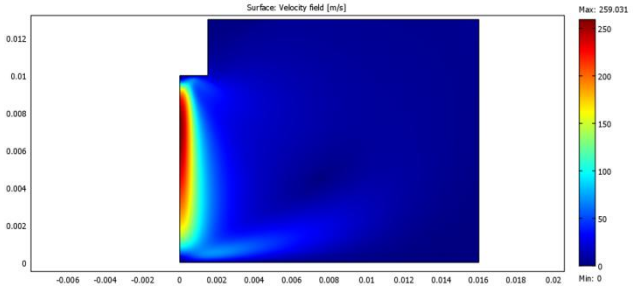


Fig. 4. Velocity Distribution Obtained by our Model (Argon Arc with 200 A Arc Current and 10 mm. Arc Length) [11]

**3.1.2. Experimental Study of Haidar and Farmer (Nitrogen arc) [12]**

The maximum temperature obtained in the 200 A nitrogen arc is approximately 27000 K. Under the same conditions, our model produced a 27120 K maximum temperature (Fig. 5); this is very close to the experimental result.

Our model proved itself as an efficient tool for predicting the velocity and temperature profiles of a GTAW arc under two different shielding gases (argon and nitrogen). In succeeding sections, we will present the constricted plasma arc properties of various shielding gases under changing arc currents, arc lengths, plasma gas inlet velocity (plasma gas flow rate) and nozzle radius.

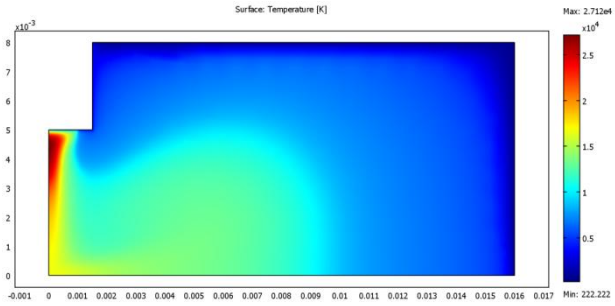


Fig. 5. Temperature Distribution Obtained by our Model (Nitrogen Arc with 200 A Arc Current and 5 mm. Arc Length). (Savaş and Ceyhun 2011)

**3.2. Argon Plasma**

Argon plasma arc is investigated with changing arc current and plasma gas flow rate. Results of the investigations with changing arc current, 6 mm nozzle to anode distance and 1.6 mm nozzle radius are given in Fig 6., results of changing plasma gas flow rate are given in Fig 7. In Fig 6a one can see that plasma velocity is higher in between the cathode-nozzle than the nozzle-anode. Doubling the arc currents doubles as well the arc velocity which can be seen from Fig.s 6a and 6c. Increasing current by 50 amperes increases arc temperatures up to 22000 and 24000 K (Fig.s 6b and 6c).

When you investigate the effects of gas inlet velocity (from 1 m/s to 7 m/s) with 8 mm nozzle to anode distance and 200-ampere arc current (Figures 7a-7g). One can easily conclude that the highest velocity makes the most stable arc. Velocity contours from cathode to nozzle and from the nozzle to anode get closer to each other. Plasma arc velocity increases gradually from 203 m/s to 238 m/s as the inlet velocity is increased by 1 m/s increments up to 7 m/s. Increasing inlet velocity also results in a very slight decrease in arc voltage.

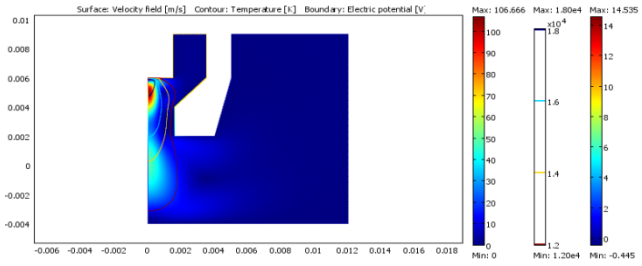


6.a

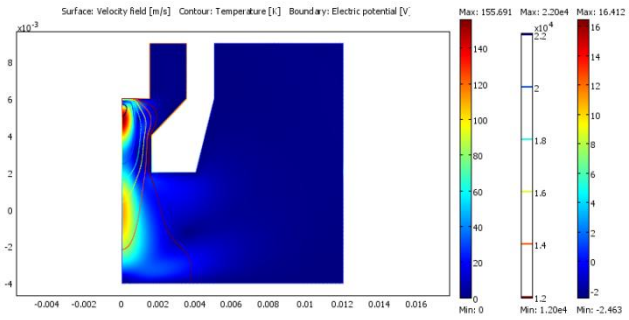


6.b

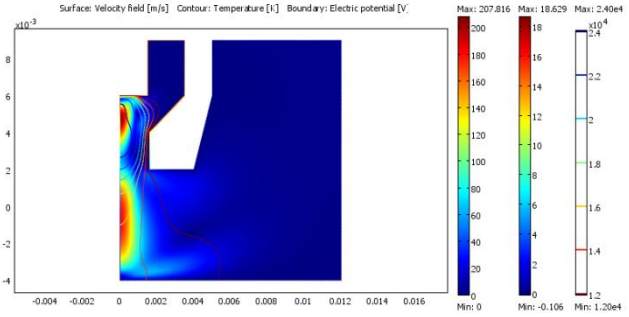


6.c.

Fig. 6. Constricted Argon Plasma Arc with Changing Arc Current and 6 mm Nozzle to Anode Distance (Nozzle Radius 1.6 mm) a. 100 A, b. 150 A, c. 200 A

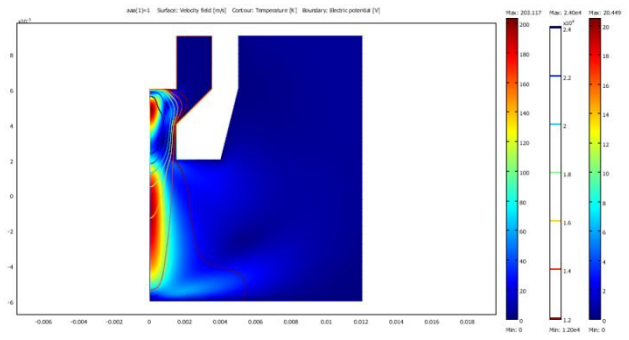

7.a.

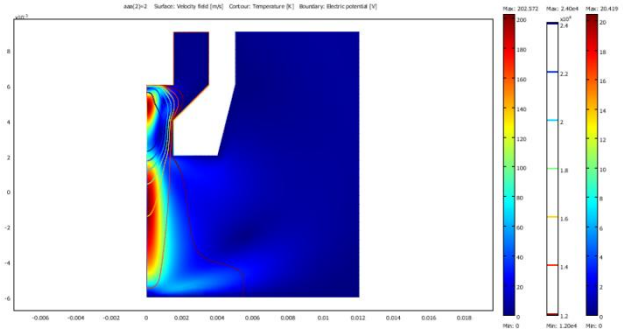

7.b.

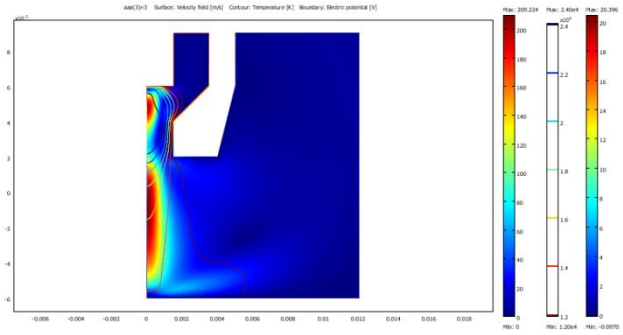

7.c.

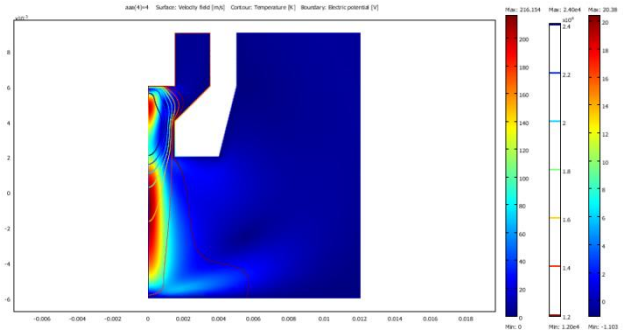

7.d.

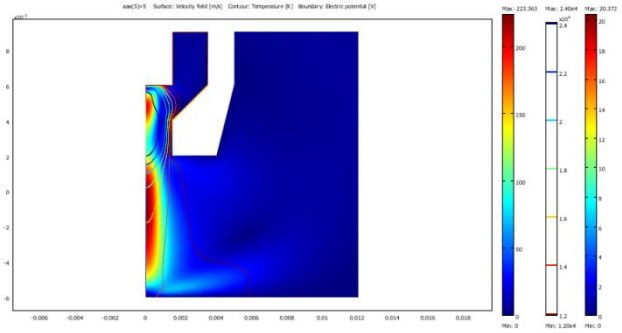

7.e

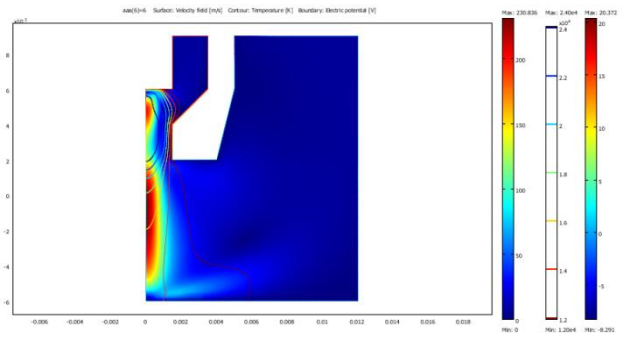

7.f.

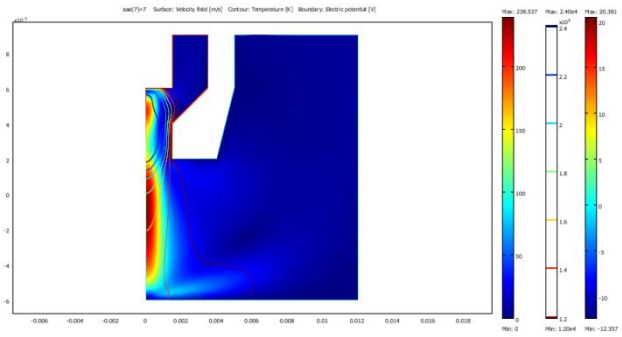

7.g.

Fig. 7. Constricted Argon Plasma Arc with Changing Plasma Inlet Velocity and 8 mm Nozzle to Anode Distance (Nozzle Radius 1.5 mm) a. 1 m/s , b. 2 m/s , c. 3 m/s, d. 4 m/s, e. 5 m/s, f. 6 m/s, g. 7 m/s

**3.3. Nitrogen Plasma**

In Fig.s 8a-8d one can find the plasma arc results for 4mm nozzle to anode distance and 100 Amperes arc current with changing nozzle radius. Physical arc constriction, in other words decreasing the nozzle radius, arguably makes the plasma velocity slower. One can expect that the plasma velocity should get higher as the

nozzle radius is decreased but the result is vice versa. Plasma arc voltage and the plasma temperature get higher as the arc is constricted.

The influence of arc constriction upon anode pressure, arc temperature, plasma velocity and arc voltage can be seen in Figs. 9a-9d. In this study, the arc current is 150 Amperes and the nozzle to anode distance is 6 mm. As the arc constriction is loosened all parameters get lower. These results conflict with the results found in Fig.8, especially for the plasma velocity. This behavior can be explained by the fact that 100 Amperes current is not high enough to cause the plasma velocity to get higher.

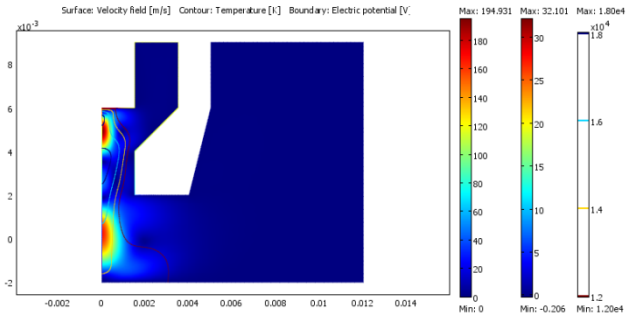


8.a.

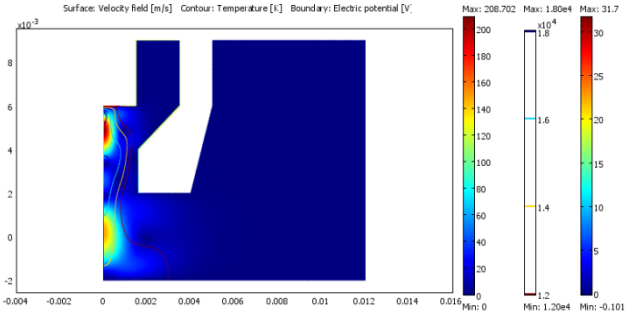


8.b.

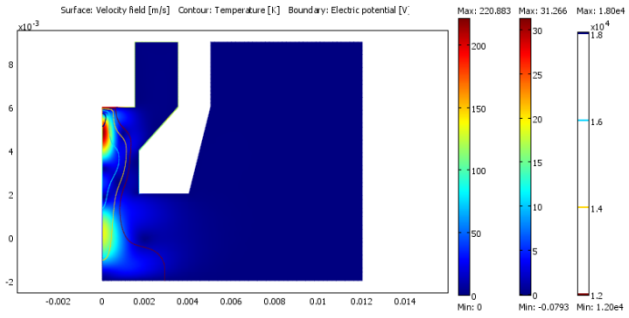


8.c.

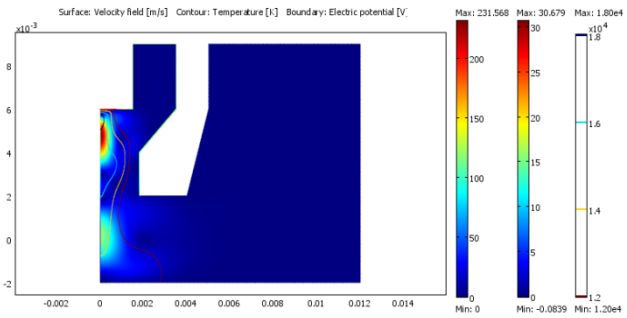


8.d.

Fig.8 Constricted Nitrogen Plasma Arc with Changing Nozzle Radius and 4 mm Nozzle to Anode Distance (Arc Current 100 A) a. 1.5 mm, b. 1.6 mm, c. 1.7 mm, d. 1.8 mm

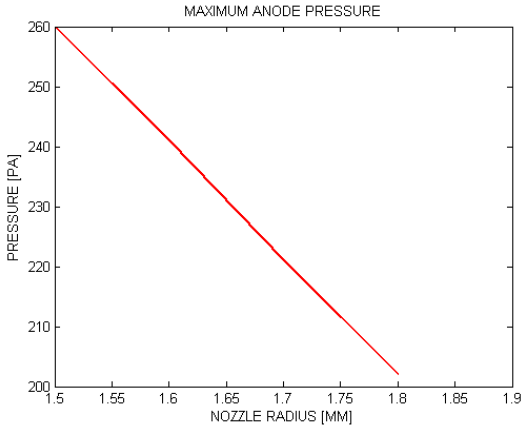


9.a.

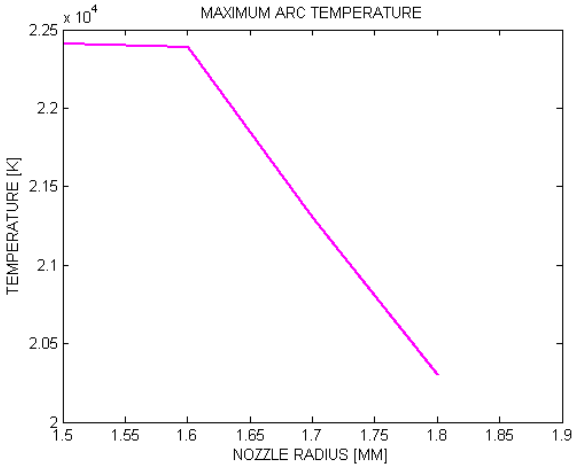


9.b.

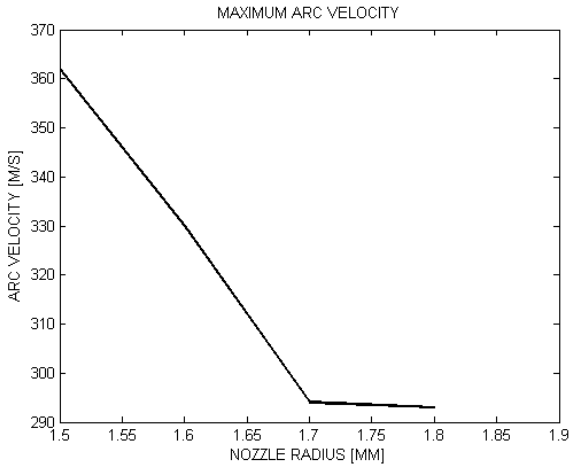


9.c.

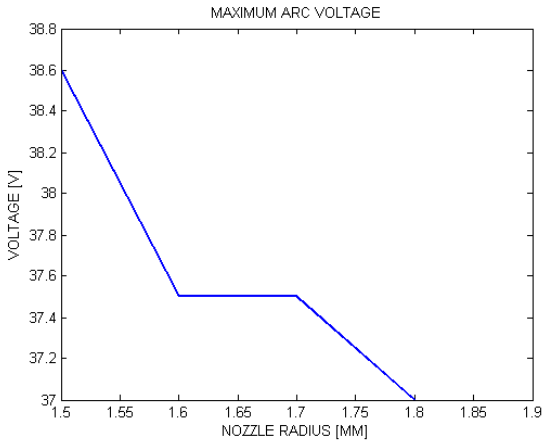


9.d.

Fig. 9. Several Parameters for Constricted Nitrogen Plasma Arc with Changing Nozzle Radius and 6 mm Nozzle to Anode Distance (Arc Current 150 A) a. maximum anode pressure, b. maximum temperature, c. maximum velocity, d. maximum arc voltage

**3.4. Air Plasma**

The physically constricted air plasma arc is also investigated with a changing nozzle radius from 0.9 mm to 1.8 mm. Figure 10 depicts several parameters for air arc with 200 Amperes arc current and 6 mm nozzle to anode distance. In Fig. 10.a maximum anode pressure decreases almost linearly from 1000 Pascal to 350 Pascal, in Fig 10.b maximum arc temperature varies between 33.000 K and 23.000 K. The relation can be named as a linear relation again. Figure 10.c shows the maximum plasma velocity, it gets the values from 900 m/s to 360 m/s. Figure 10.d shows the maximum voltage attained when the nozzle radius is enlarged. The almost linear relation between the nozzle radius and the voltage says that voltage decreases up to 33 Volts with the largest nozzle radius from the value 46 with the narrowest nozzle radius.

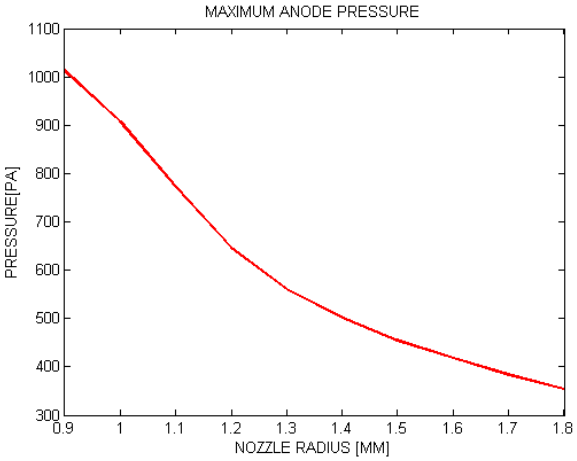
MAXIMUM ANODE PRESSURE
PRESSURE[PA]
NOZZLE RADIUS [MM]

10.a

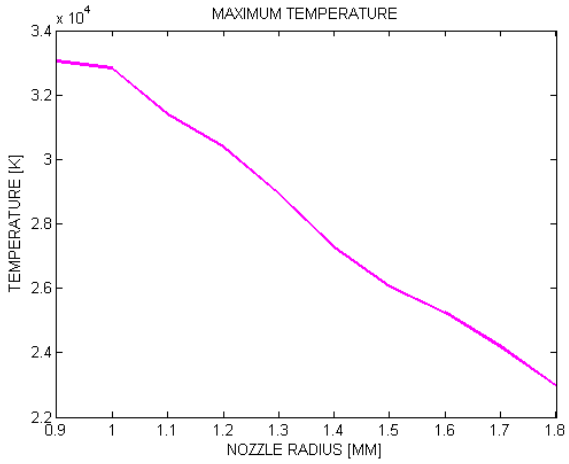
MAXIMUM TEMPERATURE
x 10^4
TEMPERATURE [K]
NOZZLE RADIUS [MM]

10.b.

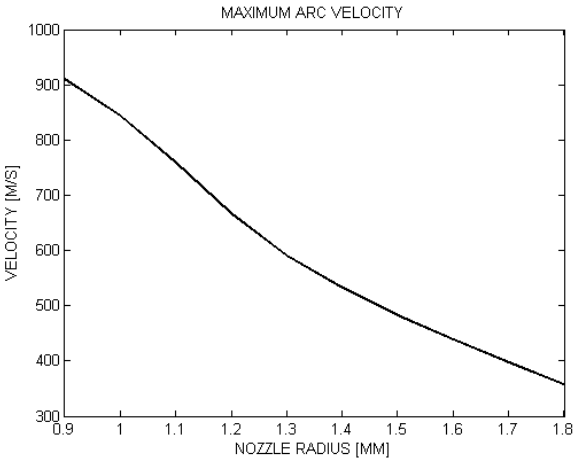
MAXIMUM ARC VELOCITY
VELOCITY [M/S]
NOZZLE RADIUS [MM]

10.c.

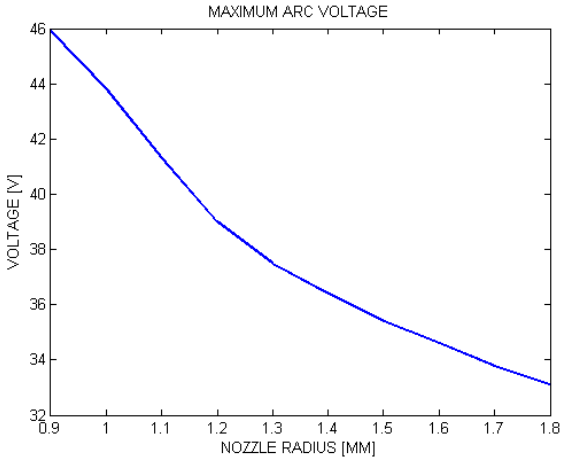


10.d.

Fig. 10. Several Parameters for Constricted Air Plasma Arc with Changing Nozzle Radius and 6 mm Nozzle to Anode Distance (Arc Current 200 A) a. maximum anode pressure, b. maximum temperature, c. maximum velocity, d. maximum arc voltage

## 4. Conclusions

4.1 A 2-D axisymmetric numerical model was established by COMSOL to study the temperature and velocity profiles of the physically constricted plasma arcs under different shielding gases.

4.2 The calculated temperature profile and the maximum plasma velocity under argon shielding gas and the maximum temperature of nitrogen arc were compared to the experimental results found in the literature. The comparisons showed good agreement. Although a comparison between the constricted arcs cannot be made since there are no experiments in the literature, the comparison of free argon and nitrogen arcs can easily be utilized to validate our model.

4.3 The computed plasma velocity profile showed good agreement when compared to the numerical results in the literature.

4.4 As the plasma arc current doubles in the argon arc the plasma velocity also doubles.

4.5 Again for argon arc, plasma arc velocity increases as the inlet plasma gas velocity is increased. Increasing inlet velocity also results in a very slight decrease in arc voltage

4.6 The most stable argon plasma arc was obtained with the maximum air inlet velocity.

4.7 When we investigate the nitrogen arc, we find out that the arc constriction can cause a drop in the plasma velocity. This may be explained by the fact that the arc current is low.

4.8 For the nitrogen arc one can also say that plasma arc voltage and the plasma temperature get higher as the nozzle is constricted.

4.9 The influence of nitrogen arc constriction upon anode pressure, arc temperature, plasma velocity and arc voltage are all positive; i.e. as the arc is constricted, these parameters are increased.

4.10 The air arc could be more thoroughly investigated. The arc constriction upto 0.9 mm nozzle radius was also computed. Plasma arc velocity and plasma voltage is increased with increasing inlet velocity.

4.11 The most stable air plasma arc was obtained with the minimum air inlet velocity.

4.12 These findings can easily be utilized for designing plasma arc torches.

## References

[1]. Aguilar J.G., C.P. Sanjurjo, A.R. Yunta and M.A.G. Calderon, 1999 "A theoretical study of a cutting air plasma torch" In IEEE transactions on plasma science 27 (1) 264–271
[2]. Hsu K.C., K. Etemadi and E.Pfender, 1983 "Study of the free burning high-intensity argon arc", In J. Phys. D: Appl. Phys. 54 (3) 1293-1301
[3]. McKelliget J. and J.Szekely, 1986 "Heat transfer and fluid flow in the welding arc" Metallurgical Transactions A Volume 17A 1139-1148
[4]. GoodarziM. , R. Choo and J.M. Toguri, 2004 "The effect of the cathode tip angle on the GTAW arc and weld pool I. Mathematical model of the arc" In J. Phys. D: Appl. Phys. 30 2744–2756.
[5]. Ramirez M.A., G. Trapaga and J. McKelliget, 2004 "A comparison between different numerical formulations for welding arc representations", In Journal of Material Processing Technology, 155-156 1634-1640
[6]. Wu C.S. , M. Ushio and M. Tanaka, 1997 "Analysis of the TIG welding arc behavior", Computational Materials Science 7 308-314
[7]. Murphy A.B. , M. Tanaka, K. Yamamoto, S. Tashiro, T. Sato and J.J. Lowke, 2009 "Modeling of thermal plasmas for arc welding: the role of the shielding gas properties and of metal vapor", J. Phys. D: Appl. Phys. 42 194006 (20pp)
[8]. Yin F. , S. Hu, C. Yu and L. Li, 2007 "Computational simulation for the constricted flow of argon plasma arc", In Computational Materials Science, 40 (3) 389-394
[9]. Boulos M.I, P. Fauchais and E. Pfender, 1994 Thermal Plasmas- Fundamentals and Applications, vol.1, Plenum, New York, pp. 388-447
[10]. Evans D.L. and R.S. Tankin, 1967 "Measurement of emission and absorption of radiation by an argon plasma",In Phys. Fluids 10 (6) 1137-1144
[11]. Savaş A. and V. Ceyhun, 2011 "Finite element analysis of GTAW arc under different shielding gases", In Computational Materials Science, 51 53-71
[12]. Haidar J. and A.J.D. Farmer, 1993 "Temperature measurements for high-current free-burning arcs in nitrogen", In J. Phys. D: Appl. Phys. 26 1224-1229